Science of the Total Environment 930 (2024) 172736

Contents lists available at ScienceDirect

Science of the Total Environment

journal homepage: www.elsevier.com/locate/scitotenv

The impact of bioaerosol trajectories on microbial community assembly and physicochemical dynamics in the atmosphere

Jin-Kyung Hong [a,1], Yongjoo Choi [b,1], Seokhyun Ahn [a], Jeonghwan Kim [b], Dong Jin Yang [b], Jongwon Heo [c], Jae-Chang Cho [b], Tae Kwon Lee [a,*]

[a] Department of Environmental and Energy Engineering, Yonsei University, Wonju, Republic of Korea
[b] Department of Environmental Science, Hankuk University of Foreign Studies, Yongin, Republic of Korea
[c] Gyeonggi-do Institute of Health & Environment, Suwon, Republic of Korea

HIGHLIGHTS

- Microbial diversity in $PM_{2.5}$ was influenced by varying aerial routes.
- Geographic and chemical factors play a crucial role in microbial community assembly.
- Community assembly in $PM_{2.5}$ was stochastic over ocean and deterministic in arid soil.
- *Pirellula* and *Nocardiopsis* were indicators of aerial routes from distinct origins.

GRAPHICAL ABSTRACT

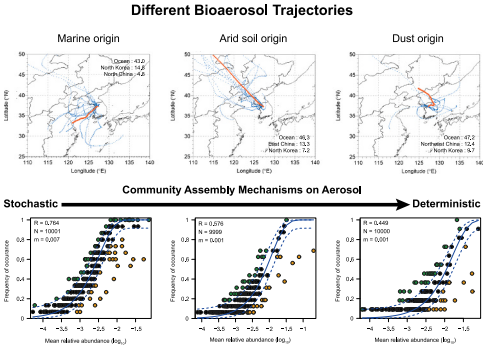

ARTICLE INFO

Editor: Pavlos Kassomenos

Keywords:
Bioaerosol
Backward trajectory
Community assembly
Neutral community model

ABSTRACT

This study explored the assembly mechanisms and physicochemical dynamics of microbial communities within atmospheric bioaerosols, focusing on the influence of different aerial trajectories. Over two years, samples near Seoul were classified into 'North', 'Southwest', and 'Others' categories based on their aerial trajectories. Physicochemical analysis of the $PM_{2.5}$ particles revealed distinct ion compositions for each cluster, reflecting diverse environmental influences. Microbial community analysis revealed that shared dominant bacterial phyla were present in all clusters. However, distinct taxonomic profiles and biomarkers were also evident, such as coastal bacteria in the 'Southwest' cluster correlating with wind speed, and arid soil-originated bacteria in the 'North' cluster correlating with cations. These findings demonstrate that biomarkers in each cluster are representative of the distinct environments associated with their aerial trajectories. Notably, cluster 'Southwest' the highest microbial diversity and a strong alignment with the neutral community model, suggesting a large influence of passive dispersal from marine environments. Contrarily, 'North' and 'Others' were more influenced by niche-dependent factors. This study highlights the complex interplay between environmental factors and microbial dynamics in bioaerosols and provides important insights for environmental monitoring and public health risk assessment.

* Corresponding author.
E-mail address: tklee@yonsei.ac.kr (T.K. Lee).
[1] These two authors equally contributed to this work.

https://doi.org/10.1016/j.scitotenv.2024.172736
Received 29 January 2024; Received in revised form 9 April 2024; Accepted 22 April 2024
Available online 23 April 2024

1. Introduction

Microbial community assembly has been a focus of ecological research, providing insights into the factors that shape bacterial community structure in complex environments, including soil and aquatic systems (Tripathi et al., 2018; Wang et al., 2020). These studies have built a crucial foundation for elucidating the influence of deterministic and stochastic factors on the shape of microbial communities, thereby providing a framework for interpreting microbial diversity and function. However, few relevant studies have focused on the atmospheric environment, particularly bioaerosols. This research gap is significant because the atmosphere is a complex and transient environment determined by the convective mixing of bacterial communities from different geographical origins (Zhai et al., 2018). This indicates that stochastic processes can significantly affect the assembly of microbial communities in the atmosphere (Zhao et al., 2022). However, conclusive empirical evidence supporting this hypothesis is lacking.

The lack of research on bacterial community assembly in bioaerosols is not just an academic deficiency but has far-reaching implications for our understanding of environmental science and public health. Airborne bacteria can serve as agents for disease transmission and can significantly impact air quality (Duchaine and Roy, 2022). Potentially infectious bioaerosols are relevant to a broad array of pathogens, including those that are endemic and can cause rare infections and outbreaks such as *Mycobacterium tuberculosis* and *Legionella pneumophila* (Hamilton et al., 2018; Wurie et al., 2016). Anthropogenic activities have a demonstrable impact on airborne microbial ecosystems, particularly increasing the richness and diversity of communities and the relative abundance of potential pathogenic organisms (Jiang et al., 2022). Furthermore, increased mortality rates from respiratory diseases correlate positively with the presence of specific pathogenic genera, particularly *Acinetobacter*, *Corynebacterium*, *Mycobacterium*, and *Staphylococcus*, suggesting a public health impact of anthropogenic influences on airborne microbial communities. Therefore, the study of the mechanisms underpinning the formation of microbial communities in atmospheric environments is not simply an extension of existing theory of microbial ecology, but a critical missing piece in a puzzle with significant social consequences, thus providing a basis for future interventions in the public health sector.

Geographic origin may serve as a noticeable factor influencing the microbial community structure in bioaerosols through localized abiotic and biotic conditions such as humidity, temperature, vegetation, and other microbial and host interactions (Zhai et al., 2018). Bioaerosols experience a "journey" through the atmosphere, and their microbial constituents may undergo significant shifts through microbial interactions, attachment on particulate matter (PM) (Gong et al., 2020), and adaptation to varying atmospheric conditions (Smets et al., 2016). Such movements may involve complex microbial interactions, such as competition, cooperation, and niche partitioning (Dussud et al., 2018; Peipoch et al., 2019), imposing both biotic and abiotic selection pressures that may generate deterministic microbial assemblage patterns. In contrast, the following passive dispersion of microbial cells on the surface of bioaerosols, the assembly of the microbial community may occur in a stochastic manner, driven by processes such as colonization, reproduction, mortality, and speciation (Zhou and Ning, 2017). Although the geographic origins of bioaerosol composition have been researched, the specific mechanisms underlying microbial community assembly during aerial transit remain under-researched.

In this study, we investigated the microbial community structure and physicochemical properties of atmospheric bioaerosols. Using back-trajectory analysis, we categorized bioaerosols based on three distinct aerial trajectories to test the hypothesis that varying geographic origins result in substantial differences in both physicochemical characteristics and microbial assemblages. To further disentangle the underlying drivers of community assembly, we employed neutral community model analyses to quantify the roles of deterministic and stochastic forces in shaping these microbial communities. We argue that the balance between deterministic and stochastic factors is influenced by the geographical origin and aerial trajectories of the bioaerosol samples. Our study provides fundamental insights into the mechanism of the microbial community assembly in bioaerosols, thereby providing a framework for future air quality risk assessment.

2. Materials and methods

2.1. Sample collection

Total of 60 samples were collected on the roof of a 5-story building (37.34°N, 127.27°E, 167 m above sea level, 20 m above ground level), approximately 35 km southeast of Seoul, from October 2016 to April 2018. The sampling site was in a rural area with low-rise buildings and scattered farmland, as well as a four-lane road and a river, while the eastern side of the site was a rising valley. $PM_{2.5}$ was sampled using low-volume sampler (16.7 LPM) consists of a cyclone (2.5 μm size cut, URG-2000-30EH) and single stage filter package. Three different types of filters were used for each purpose. Polytetrafluoroethylene (PTFE) membranes (Pall, Port Washington, USA) and quartz microfiber (Whatman, Kent, UK) filters were used to analyze the total mass/ion concentration and carbonaceous aerosol concentration, respectively. A polycarbonate (PC) membrane filter (Merck Millipore, Massachusetts, USA) was used to isolate DNA from microorganisms associated with $PM_{2.5}$. Before the $PM_{2.5}$ sampling, the PTFE filter was dried in desiccator (relative humidity at ~40 %) for 24 h and quartz filter was pre-baked at 550 °C for 4 h to remove organic carbon residues. For microbiological purposes, $PM_{2.5}$ was collected on the PC membrane filter for 72 h (3 days), and the filter was replaced when the flow rate fell below 10 L/min. The remaining two filters for chemical analysis were replaced every 24 h during the 72 h bioaerosol sampling period. After sampling, the quartz filter was wrapped in an aluminum foil and stored at −20 °C while PTFE and PC membrane filter was immediately subjected to further analyses.

2.2. Analysis of $PM_{2.5}$ chemical composition

The mass concentration of $PM_{2.5}$ was determined by weighing the PTFE filter before and after sampling. The filtered PTFE filter was soaked in a 15 mL solution of 1 mL ethanol and 14 mL distilled water and then sonicated for 30 min to dissolve the soluble ions. Impurities in the samples were removed by syringe filtration. The concentrations of the three anions (Cl^-, NO_3^-, and SO_4^{2-}) and five cations (Na^+, NH_4^+, K^+, Mg^{2+}, and Ca^{2+}) were determined by ion chromatography (IC; Advanced Modules, Metrohm). The cations were analyzed using a Metrosep C4-150/4.0 column with 4 mM HNO_3 as an eluent, and for anion analysis, a Metrosep A Supp 5-150/4.0 column with 3.2 mM Na_2CO_3 and 1.0 mM $NaHCO_3$ were used. The minimum detection limits for IC analysis were determined by repeatedly analyzing the standard solutions of the minimum concentrations used for IC calibration seven times. The values in μg/L (with uncertainties in parentheses as %) were 4.4 (2.0) for Cl^-, 9.8 (2.7) for NO_3^-, 8.1 (2.2) for SO_4^{2-}, 6.2 (3.1) for Na^+, 11.9 (6.1) for NH_4^+, 14.1 (5.1) for K^+, 10.3 (3.6) for Mg^{2+}, and 5.3 (6.5) for Ca^{2+}.

A quartz filter for organic carbon (OC) and elemental carbon (BC) analysis was used after baking overnight at 450 °C. OC and BC were analyzed according to National Institute of Occupational Safety and Health (NIOSH) Method 5040 using thermal optical transmission (TOT).

2.3. Backward trajectory analysis and meteorological data

Three-dimensional air mass transport pathways were calculated using the Hybrid Single Particle Lagrangian Integrated Trajectory (HYSPLIT) model version 4 (Draxler et al., 2018). Meteorological data were obtained from the Global Data Assimilation System (GDAS; 1° ×

1°) as inputs to the HYSPLIT model. The starting altitude and time for the backward trajectory calculations were 500 m above ground level (a.g.l.) at the receptor site and on the middle of the bioaerosol sampling period (~3 d), respectively. The simulation time was past 72 h, which was sufficient to consider the lifetime of the aerosols owing to dry and wet deposition (Choi et al., 2020; Kanaya et al., 2016).

To classify similar geographic origins using the backward trajectories which reflect similar chemical histories, we used an angle-based classification which is a measure of how similar two back trajectory points are in terms of their angle from the starting location of the back trajectories (Carslaw, 2019). Air-mass origins were distinguished using an R function, calculating clusters for back trajectories (trajClust) included in the 'openair' R package. The optimal number of clusters was selected into three such as North, Southwest, and Others. With an increase of the number of clusters to four, 'other' cluster was divided into two clusters, whose distances were long and short each. The last division appeared to be relatively insignificant, so three was chosen as the optimum number of clusters.

Seasons for the samples were defined as follows: Spring encompasses March to May; Summer, June to August; Fall, September to November; and Winter, December to February. Meteorological parameters were obtained from the Suwon Weather Station (SWS; 37.27°N, 126.98°E, 34.5 m asl; see Fig. 1 for the location), about 26 km to the west-southwest. These had the highest correlation with the on-site data from the automatic weather station compared with those from nearby weather stations (Lee et al., 2016).

2.4. DNA extraction and quantitative qPCR

gDNA was extracted from the PC membrane filters using a minor modification of a previously described method (Jiang et al., 2015). After aerosol sampling, the PC membrane filter was incubated in 5 mL PBS (phosphate buffer saline) at 60 °C for 2 h for better DNA recovery by inactivating nuclease activity. The following steps were carried out using a MO-BIO PowerSoil DNA isolation kit (Carlsbad, CA, USA) according to the manufacturer's instructions. The sample volume used in the experiment was 5 mL, which exceeds the specified maximum capacity of 1 mL. Accordingly, the quantity of bead material and reagents was increased fivefold, and the final elution volume was adjusted to 50 μL. The quantity and purity of the gDNA were measured using the NanoDrop 2000 spectrophotometer (Thermo Fisher Scientific, Wilmington, DE, USA), and 42 samples with DNA concentration above 5 ng/μL were used. Extracted gDNA samples were stored at −80 °C until analysis.

Bacterial abundance was quantified through the assessment of 16S rRNA gene copy numbers, employing quantitative PCR with the bacterial universal primer set EUB338F (5′-ACTCCTACGGGAGGCAGCAG-3′) and BAC515R (5′-TTACCGCGGCKGCTGGCAC-3′). qPCR procedures, including amplification, signal normalization, and copy number calculation, were performed using the same methods as those used in previous study (Hong and Cho, 2015).

2.5. Bacterial 16S rRNA sequencing and sequence analyses

The V3-V4 region of the bacterial 16S rRNA gene was amplified using 338F (5′-ACTCCTACGGGAGGCAGCAG-3′) and 806R (5′-GGACTACHVGGGTWTCTAAT-3′) primers with overhang adapter sequences which are compatible with Illumina index and sequencing primers. Index PCR, library pooling, and sequencing were performed on an Illumina MiSeq platform (Illumina, San Diego, USA) and at Macrogen Inc. (Seoul, Republic of Korea). The 16S rRNA gene sequence data were processed using the Quantitative Insights into Microbial Ecology (QIIME 2020.8) program (Bolyen et al., 2019). Paired-end reads were joined and demultiplexed using plugins in QIIME. The reads were subjected to quality control using a three-step process. First, the sequences were filtered based on the Phred minimum quality score (> 10) and the maximum number of ambiguous sequences (< 6). Near-error-free and maximum 450 bp length sequences were obtained based on the Illumina error profile using Deblur (Amir et al., 2017). Finally, sequences classified as *Archaea*, mitochondria, or chloroplasts were excluded from analysis. Using the subsampled open reference operational taxonomic unit (OTU) clustering approach (Rideout et al., 2014) with the SILVA (release 138) reference database, sequences showing >97 % identity with the mapped reference sequences were clustered into a single OTU, and the representative feature sequence per OTU was retrieved. Only OTUs with a relative abundance of ≥0.05 % in at least one sample remained in the dataset. The sequence data used in this study are available in the NCBI SRA (Sequence Read Archive) database under accession number PRJNA749884.

2.6. Statistical analyses

All statistical analyses and visualizations were performed using R software (ver. 4.2.1) packages, and vegan (ver. 2.6-4) software (Oksanen et al., 2019). Alpha diversity metrics, including species richness and Shannon's diversity index, were calculated using the OTU relative abundance table and the taxonomic positions of feature sequences were classified using a scikit-learn multinomial naïve Bayesian classifier trained using SILVA reference sequences (Bokulich et al., 2018). Differences in bacterial community composition between clusters were visualized using non-metric multidimensional scaling (nMDS) based on the Bray-Curtis dissimilarity matrix, and the significance of these

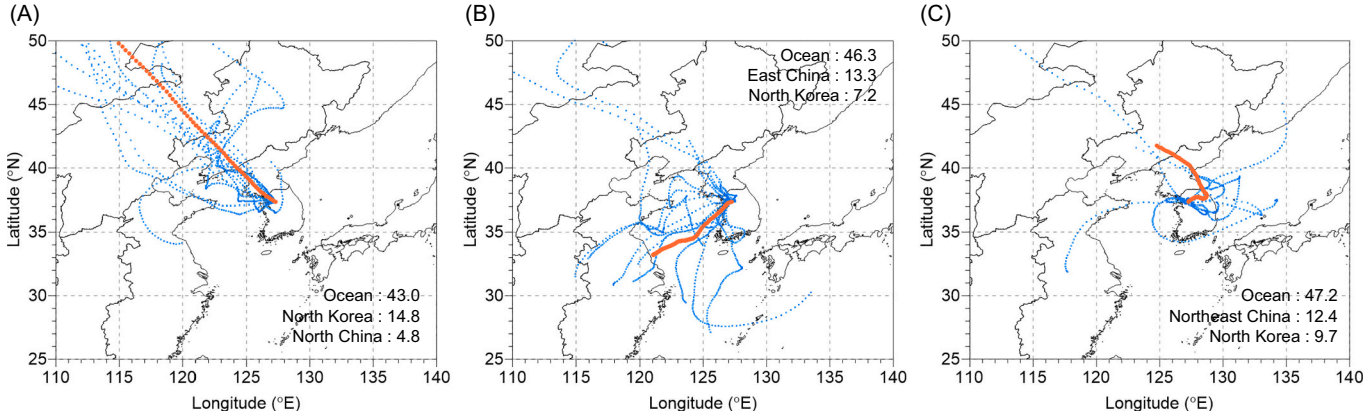

Fig. 1. Using angle-based cluster from 'openair' package in R, the mean three days backward trajectory (BT) of each sample, based on the middle of the sampling periods, was calculated using HYSPLIT model and meteorological data of the GDAS 1°. Samples were grouped into three BT-clusters (a, b, and c, respectively) and the clusters were designated as N (North), S (Southwest), and O (Others).

differences was tested using Analysis of Similarities (ANOSIM) with 999 permutations. The envfit function of the vegan package was used to calculate the correlation between significant variables and microbial communities.

A normality test was conducted using the Shapiro-Wilk test to assess the distribution of the variables. Depending on the normality of the data, either analysis of variance (ANOVA) or the Kruskal-Wallis test was employed to evaluate the significance of the differences observed among the variables. The significance of pairwise differences was also tested using Tukey's HSD or the MCTP test according to normality. The Spearman's rank correlation coefficient was used to determine the correlation between variables.

The neutral community model was calculated at the genus level to test the contribution of stochastic processes in shaping bacterial community assembly using the minpack.lm package in R (Chen et al., 2019; Sloan et al., 2006). The 95 % confidence intervals for all goodness of fit statistics were calculated using 1000 bootstrap replicates. Linear discriminant analysis effect size (LEfSe) analysis was performed to identify the significant biomarker genera using 'microbiomeMarker' package in R (Segata et al., 2011). Differently abundant bacterial groups were defined using an LDA score ($\log_{10}$) of >4. The Kruskal-Wallis test ($P < 0.05$) or pairwise Wilcoxon test ($P < 0.05$) was applied as a factorial test for the classes.

3. Results

3.1. Bioaerosol clustering by aerial trajectories and $PM_{2.5}$ properties

Using back-trajectory analysis, we classified bioaerosols into three groups based on their aerial trajectories (Fig. 1). They were designated as 'N (North, n=16)', 'S (Southwest, n=15)', and 'O (Others, n=11)'. Notably, all three clusters had a significant portion of their trajectories over oceanic areas (43.0 %, N: 46.3 %, S: 47.2 %, O) (Fig. 1). In terms of geographic influence, while the North Korean region affected clusters N and O, they also traversed different regions in northern China and Northeast China for clusters N and O (Fig. 1A and C), respectively. In contrast, cluster S was predominantly influenced by East China (Fig. 1B). Clusters N, S, and O predominantly consisted of samples collected in

Table 1
Physico-chemical characteristics of $PM_{2.5}$ according to its aerial route.

		N[a] (n = 16)	S (n = 15)	O (n = 11)	Significance[b] (P value)
Seasons (Spring; Summer; Fall; Winter)		3; 0; 3; 10	1; 0; 10; 4	6; 1; 4; 0	n.a.
Meterological variables	Temperature (°C)	2.1 ± 6.9[c,*]	8.4 ± 6.9[†]	13.0 ± 6.7[†]	< 0.05
	Precipitation (mm/d)	0.5 ± 1.0	0.5 ± 0.9	0.4 ± 0.7	0.9
	Wind speed (m/s)	2.0 ± 0.7	1.6 ± 0.5	1.9 ± 0.7	0.3
	Relative humidity (%)	60.3 ± 9.8	67.3 ± 12.8	68.3 ± 8.8	0.1
Chemical variables (proportional to $PM_{2.5}$ mass)	Mass concentration ($\mu g/m^3$)	(3.3 ± 1.2) × 10	(3.8 ± 8.6) × 10	(3.7 ± 2.0) × 10	0.1
	OC	31.6 ± 15.6%[d]	26.2 ± 6.4%	27.8 ± 10.4%	0.9
	EC	3.3 ± 2.1%	2.8 ± 0.8%	3.4 ± 1.4%	0.5
	Cl^-	2.2 ± 1.3%	2.4 ± 1.9%	0.9 ± 1.0%	0.1
	NO_3^-	22.5 ± 9.8%[*]	19.6 ± 6.9%[*]	12.1 ± 9.6%[†]	< 0.05
	SO_4^{2-}	13.1 ± 4.6%	15.8 ± 5.7%	20.4 ± 9.0%	0.1
	Na^+	0.2 ± 0.8%[*]	0.7 ± 3.6%[*,†]	1.8 ± 3.7%[†]	< 0.05
	NH_4^+	12.6 ± 2.0%[*]	12.4 ± 4.0%[*,†]	10.3 ± 3.2%[†]	< 0.05
	K^+	1.2 ± 0.3%[*,†]	1.1 ± 0.2%[*]	1.5 ± 0.5%[†]	< 0.05
	Mg^+	0.3 ± 0.2%	0.3 ± 0.2%	0.9 ± 1.0%	0.2
	Ca^{2+}	0.3 ± 0.3%[*,†]	0.2 ± 0.1%[*]	0.5 ± 0.4%[†]	< 0.05

[a]Clusters decided based on the backward trajectory analysis.
[b]Significance of difference tested by Kruskal-Wallis test.
[c]Mean ± standard deviation.
[d]Fraction of concentration to $PM_{2.5}$ mass concentration.
[*,†]Post hoc pairwise comparison using mctp test.

winter (62.5 %), fall (66.7 %), and spring (54.5 %) seasons, respectively (Table 1). While other meteorological parameters did not differ by aerial route, N, which was sampled at a higher rate in winter, had significantly lower temperatures compared to S and O (Table 1).

The physicochemical properties of $PM_{2.5}$ along the aerial route were compared (Table 1). Mass concentrations ($\mu g/m^3$) and OC proportions of $PM_{2.5}$ were not significantly different between samples (Kruskal-Wallist test, $P > 0.05$). In the ionic physicochemical indicators, the proportions of NO_3^-, Na^+, NH_4^+, K^+, and Ca^{2+} in $PM_{2.5}$ were significantly different between samples along the aerial route (mctp test, $P < 0.05$). NO_3^- emerged as the dominant species within both cluster N (22.5 ± 9.8 %) and cluster S (19.6 ± 6.9 %), whereas the proportion of NO_3^- in O (12.1 ± 9.6 %) was significantly low. The proportional concentration of NH_4^+ in N (12.6 ± 2.0 %) was significantly higher compared to cluster O (10.3 ± 3.2 %) (Table 1). For minor constituents of $PM_{2.5}$, significant differences in the proportional concentrations of K^+, Na^+, and Ca^{2+} were evident across clusters, with the highest concentrations of these ions found within O. The back-trajectory analysis revealed that bioaerosols in this study can be divided into three distinct clusters with different ionic composition of $PM_{2.5}$ along the aerial trajectories.

3.2. Comparing bacterial diversity across different aerial trajectories

We compared the bacterial diversity in $PM_{2.5}$ by aerial trajectories. DNA concentrations and 16S rRNA gene copy numbers showed no significant differences between clusters (Fig. 2A and B; Kruskal-Wallis test, $P > 0.05$). In total, 824,747 quality-filtered sequences were obtained and classified into 4801 OTUs. Both alpha-diversity indices in S (7.1 ± 1.0, Shannon; 323.9 ± 84.0, richness) were significantly higher (mctp test, $P < 0.05$) than those in N (4.6 ± 2.2; 100.1 ± 90.3) and O (5.0 ± 0.9; 72.7 ± 21.3) (Fig. 2C and D). Although the total amount of microorganisms in $PM_{2.5}$ did not differ between clusters according to aerial route, the bacterial diversity of S was particularly high.

To pinpoint the effects of meteorological and chemical parameters on bacterial diversity, correlation coefficients were calculated, and the results showed distinctive relationships according to the aerial trajectories (Fig. S1). Bacterial abundance of cluster N showed significantly negative correlation (Spearman, $P < 0.05$) with RH ($rho = -0.7$), NO_3^- ($rho = -0.7$), NH_4^+ ($rho = 0.6$), and OC ($rho = -0.5$) (Fig. S1). In cluster S, the alpha diversity indices were positively correlated with wind speed ($rho = 0.6$, richness) and Cl^- ($rho = 0.6$, richness; $rho = 0.6$, Shannon) (Spearman, $P < 0.05$) (Fig. S1). In cluster O, biological parameters were significantly positively correlated (Spearman, $P < 0.05$) with cations, such as Na^+ ($rho = 0.78$, bacterial abundance), Ca^{2+} ($rho = 0.66$, richness), K^+ ($rho = 0.69$, Shannon), and Mg^{2+} ($rho = 0.69$, Shannon).

To determine the differences in the microbial communities at the genus level in each cluster, we compared their beta diversity using nMDS (Fig. 3). In the nMDS plot, S was tightly clustered and was clearly separated from N and O (Fig. 3A; ANOSIM, $R = 0.27$, $P = 0.001$). The average inter-cluster distance of S to remaining two clusters were comparable (0.80 ± 0.12 for S-N; 0.78 ± 0.06 for S-O). It is noteworthy that despite O comprising samples from diverse aerial trajectories, it exhibited more cohesive clustering on the nMDS plot compared to N. We found that the two diversity indices (Shannon, $R^2 = 0.78$, $P < 0.05$; richness, $R^2 = 0.85$, $P < 0.05$) and Cl^- ($R^2 = 0.15$, $P < 0.05$) had a significant impact on this variation in beta diversity. Further examination of the inter-sample relationships on the nMDS plot with gradient shading reflecting Shannon's diversity index confirmed a division within cluster N into two groups (Fig. 3B). Although the proportion of Cl^- in $PM_{2.5}$, showed no significant differences between clusters (Table 1), it exerted a significant influence on the variability of microbial community composition within individual samples.

3.3. Dominant bacterial taxa in $PM_{2.5}$ across various clusters

All $PM_{2.5}$ samples across clusters shared three consistent bacterial

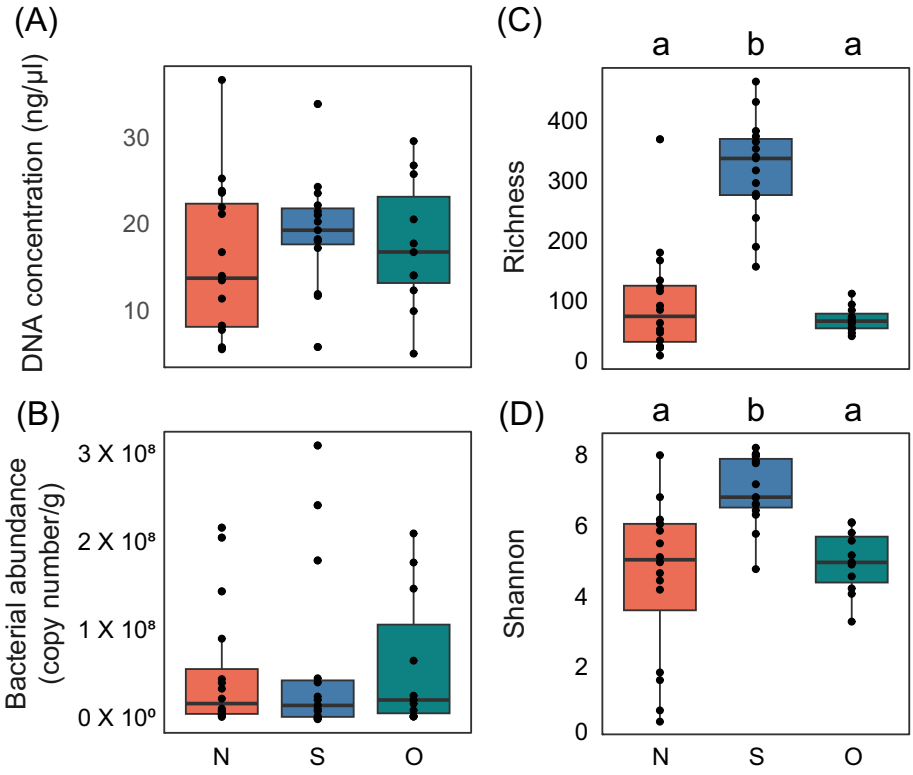

Fig. 2. Box plot displaying the variations in quantitative biological factors (A and B) and bacterial diversity indices (C and D) within the bacterial community associated with $PM_{2.5}$. The clusters labeled as N, S, and O correspond to back trajectory clusters. Lowercase letters displayed above the plots highlight significant differences ($P < 0.05$) as determined by post hoc pairwise comparisons using the mctp test.

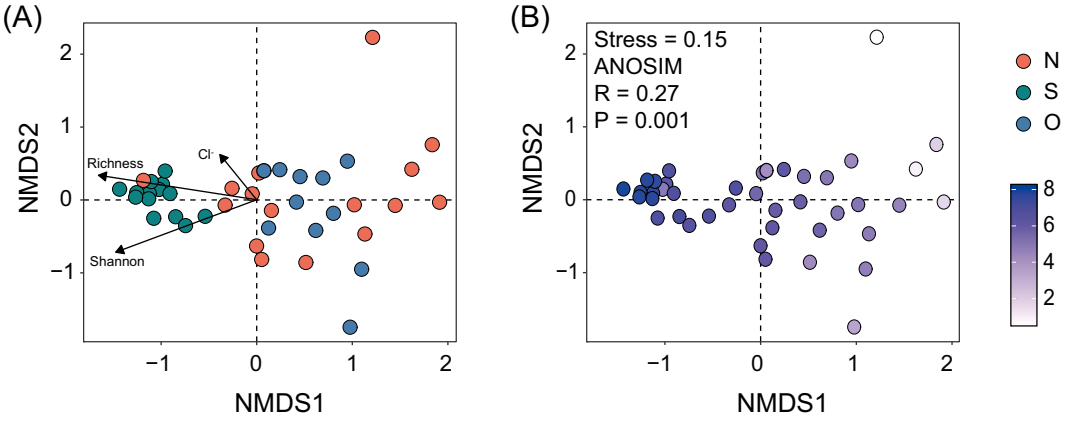

Fig. 3. Non-metric multidimensional scaling (nMDS) ordination plot based on the Bray-Curtis distance of genus-level profile of bacterial communities associated with $PM_{2.5}$. (A) Backward trajectory clusters are distinguished by color, and factors with a significant influence on the nMDS ordination are indicated by arrows. (B) Point colors correspond to Shannon's diversity values. The significance of difference was tested using ANOSIM and described in the plot background.

phyla, *Gammaproteobacteria*, *Bacteroidota*, and *Firmicutes*, as the top dominant members accounting for 65.2 (±25.8)%, 75.6 (±2.1)%, and 73.9 (±13.4)% of bacterial communities of each cluster N, S, and O (Fig. S2). The differences in the relative abundances of these phyla between clusters were not significant (Kruskal-Wallis test, $P > 0.05$). Apart from these dominant phyla, the abundance profiles of the remaining bacterial phyla demonstrated a source-specific distribution, exhibiting significant differences according to cluster (Fig. S2 and Table S1). The abundance of the phylum *Acidobacteriota* was significantly higher (Tukey's HSD test, $P < 0.05$) in cluster N than in cluster S (Table S1), mainly due to its remarkably high abundance in samples N09 (89.9 %), N05 (74.2 %), and N10 (67.6 %) (Fig. S2). The relative abundance of the phylum *Planctomycetota* in cluster S was significantly higher (mctp test, $P < 0.05$) than in the other two clusters (Fig. S2 and Table S1). The abundance of *Verrucomicrobia* was also significantly higher (mctp test, $P < 0.05$) in cluster S than in cluster N (Fig. S2 and Table S1). The phylum *Actinobacteriota* was significantly more abundant (Tukey's HSD test, $P < 0.05$) in cluster O than in cluster S (Fig. S2 and Table S1). While the dominance patterns of bacterial phyla were distinct across clusters, it is important to acknowledge that the surrounding microbial communities

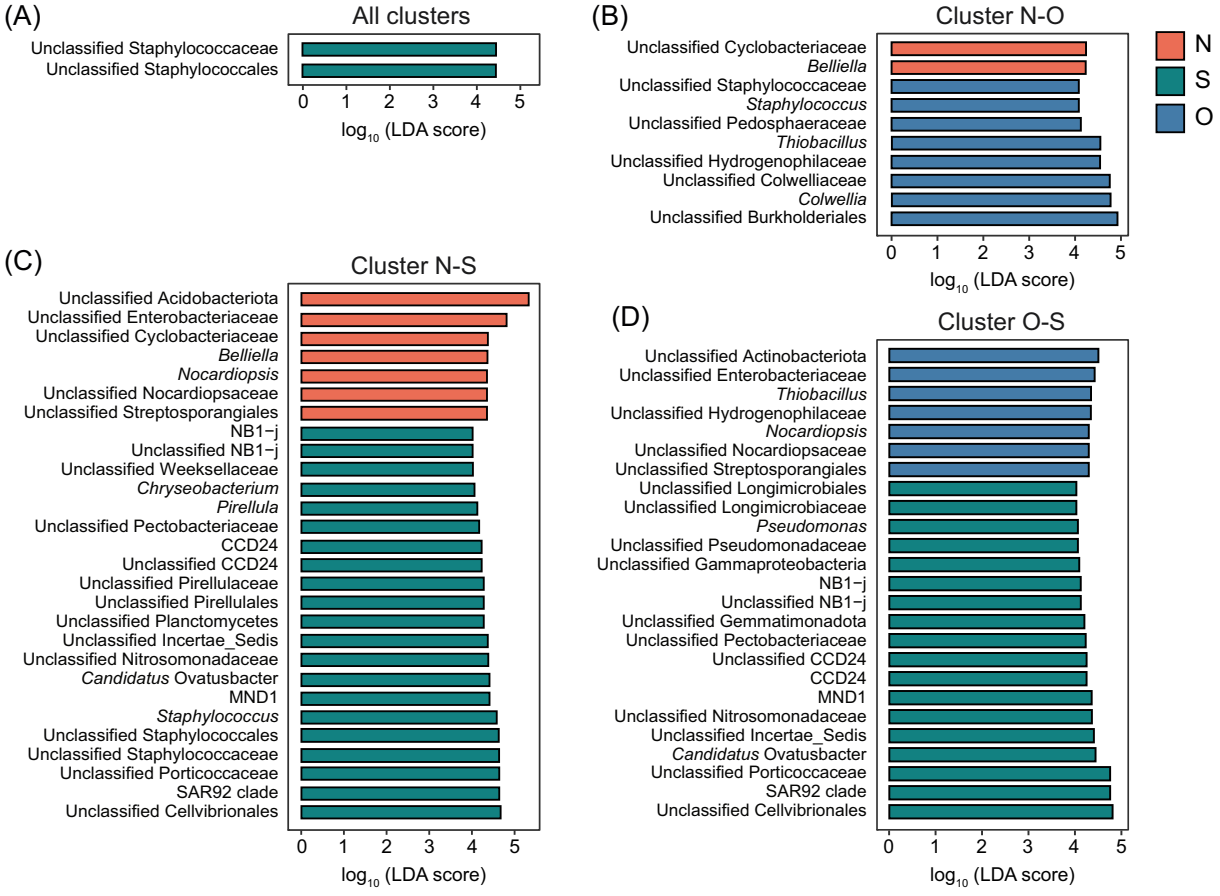

Fig. 4. LDA scores ($\log_{10}$ LDA ≥ 4) from the LEfSe analysis reflecting bacterial community distinctions. Pairwise comparisons are shown (A) across all clusters, and between (B) clusters N and O, (C) clusters N and S, and (D) clusters O and S. Bar color signifies the cluster indicated by each biomarker.

could also impact bioaerosol communities. This influence is subject to variations in aerosolization potential, which are dictated by factors such as relative humidity, wind speed, and precipitation.

Using LEfSe analysis with an LDA score above four, we identified bacterial taxa that could serve as biomarkers to distinguish between the clusters and elucidate the injection of endemic bacterial genera from the environments in each aerial route. In the pairwise comparisons, more bacterial taxa emerged as biomarkers when two individual clusters were compared to comparisons involving all three clusters (Fig. 4). In the three-cluster comparison, only two biomarkers related to *Staphylococcus* indicating S were identified (Fig. 4A). However, in the two-cluster comparisons, 10 biomarkers for N-O (2 for N; 8 for O), 28 biomarkers for N-S (7 for N; 21 for S), and 25 biomarkers for S-O (18 for S; 7 for O) were identified (Fig. 4B-D). These results revealed that cluster S had relatively more biomarkers than the other clusters. In the pairwise comparison, S was commonly enriched with 11 biomarkers, including NBJ1-j, unclassified NBJ-j, unclassified *Pectobacteriaceae*, CCD24, unclassified CCD24, unclassified Incertae_Sedis, unclassified *Nitrosomonadaceae*, *Candidatus* Ovatusbacter, MND1, unclassified *Porticoccaceae*, SAR92 clade, and Unclassified *Cellvibrionales*. N contained two different taxa, unclassified *Cyclobacteriaceae*, and *Belliella* whereas O was rich in Unclassified *Hydrogenophilaceae*. Interestingly, when O and S were analyzed pairwise with N, two and three biomarkers associated with *Staphylococcus*, respectively, were determined to be the indicators classifying these two clusters.

3.4. Microbial community assembly influenced by the aerial trajectories

The neutral community model (NCM) successfully estimated 55.4 % of the variation in the frequency of genus occurrences within the total $PM_{2.5}$ associated community (Fig. 5A). Furthermore, when extended to specific clusters, the NCM explained a larger variance in cluster S (76.4 %) (Fig. 5C), while its predictive accuracy decreased to 57.6 % and 44.9 % for clusters N and O, respectively (Fig. 5B and D). Despite the remarkable difference in the goodness of fit between clusters N and O, their mitigation rates (m), as predicted by the NCM, were comparable (Fig. 5B and D). The highest mitigation rate was observed for NMC of cluster S (Fig. 5C).

Although cluster S exhibited the highest goodness of fit for NCM, cluster O manifested the highest cumulative relative abundance (53.6 ± 17.5 %; $n = 140$) of bacterial genera which followed neutral model (Fig. S3). This was in contrast to clusters S and N, which showed 44.8 ± 8.0 % ($n = 160$) and 41.0 ± 24.4 % ($n = 166$) respectively (Fig. S3). Nonetheless, the pronounced variance within cluster O rendered this difference statistically insignificant (Kruskal-Wallis test, $P > 0.05$). In cluster N, the NCM identified an average of 50 % (± 27.7 %; $n = 23$) of the cumulative abundance of genera as under-representative outliers, while the relative abundance of under-representative genera in cluster S (25.4 ± 13.0 %; $n = 29$) was significantly (mctp test, $P < 0.05$) lower than cluster N (Fig. S3). For the over-representative genera, the cumulative abundance across the clusters was observed as cluster S (29.7 ±

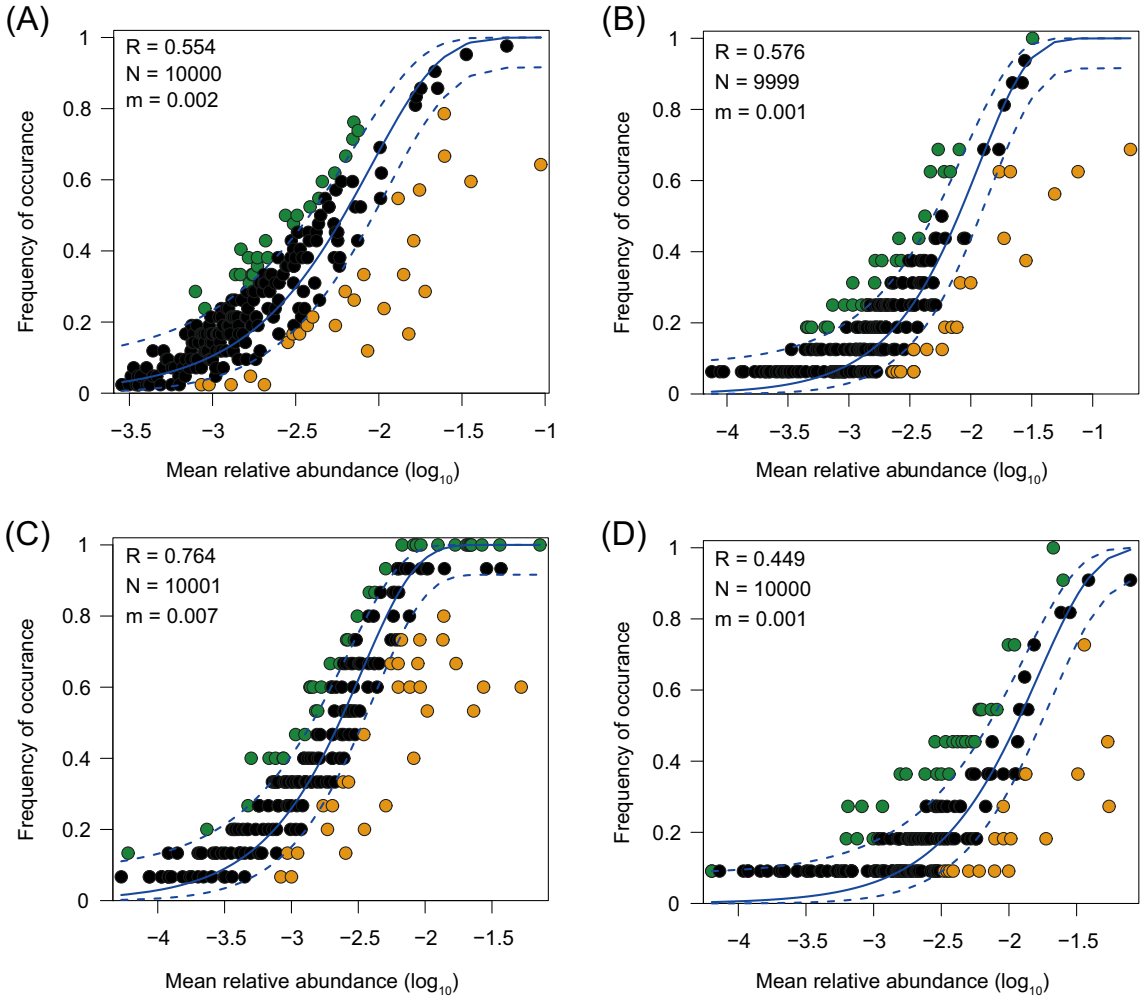

Fig. 5. Fit of neutral model for bacterial communities in (A) all, (B) cluster N, (C) cluster S, and (D) cluster O. Point represents for bacterial genus classified from sequence analysis process, and different colors indicate over- (green) and under- (yellow) representative outliers from the predicted by the neutral model. The R^2 indicates the goodness of fit to neutral model. N indicates the metacommunity size and m indicates immigration rate.

8.9 %; $n = 40$) > cluster O (16.4 ± 8.0 %; $n = 32$) > cluster N (9.0 ± 4.9 %; $n = 27$), with each cluster differing significantly from the others (mctp test, $P < 0.05$). These results highlight the complex interplay of neutral and niche-dependent forces in the assembly of bacterial communities in $PM_{2.5}$ across different aerial trajectories. In clusters S and N, a broader array of bacterial genera was dispersed, each with a lower abundance, whereas in cluster O, fewer genera were dispersed, but in higher abundance. Within cluster N, the majority of niche-dependent assembled genera appeared to be negatively influenced, in contrast to clusters S and O, which indicated a positive impact on their niche-dependent assembled genera.

3.5. Physicochemical factors influencing microbial community assembly

To evaluate the impact of the physico-chemical factors of $PM_{2.5}$ on differential community assembly, we aligned the NCM prediction status of each biomarker with its correlation coefficient with the relevant physicochemical factors (Table 2). The genus *Belliella*, a cluster N biomarker, was predicted to be under-represented in the NCM of cluster N (Table 2). Significantly, it was negatively correlated with temperature (Table 2). The genus *Nocardiopsis* was fit to NCM of cluster N; however, it was predicted to be over-representative of the NCM of cluster O. This genus showed a significant positive correlation with the Ca^{2+} levels (Table 2). Among the cluster S biomarkers, the genera *Pirellula* and *Staphylococcus* and the uncultured genus MND1 were well fitted to the NCM of cluster S. Genus *Staphylococcus* and MND1 demonstrated significant positive correlations with Na^+ and mass concentration, respectively. Genus CCD24 and *Pseudomonas* were over-representatives, while the remaining four cluster S biomarkers were under-represented in the NCM of cluster S. Notably, the genus *Pirellula* and all over-representatives showed no significant correlation with any factor (Table 2). In contrast, under-representatives, including the uncultured genus SAR92 clade, *Candidatus* genus Ovatusbacter, and *Chryseobacterium* showed significant positive correlations with major components of $PM_{2.5}$ (NO_3^-, SO_4^{2-}, NH_4^+, and OC) as well as ion components (Table 2). Both cluster O biomarkers, *Thiobacillus* and *Colwellia*, were underrepresented. While *Thiobacillus* showed significant positive correlation with SO_4^{2-}, cations (Mg^{2+}, Ca^{2+}, K^+, and Na^+), and temperature, *Colwellia* negatively correlated with SO_4^{2-} as well as NH_4^+ (Table 2). It was noted that no biomarker showed significant seasonal differences, highlighting that biomarker distribution is more influenced by aerial trajectories than by the seasons.

4. Discussion

Our results have provided a comprehensive background for the understanding of the assembly mechanisms of microbial communities associated with $PM_{2.5}$. We highlighted the complex balance between stochastic and deterministic processes that vary according to aerial trajectories. These findings significantly improve our understanding of atmospheric environment as dynamic ecological niches for microorganisms and elucidate the complex interactions between microorganisms and atmospheric environmental factors. Our research goes beyond the traditional focus on seasonal variations or nearby urban environments, as emphasized in previous studies (Feng et al., 2021; Li et al., 2023; Zhang et al., 2023; Zhou et al., 2021), to illuminate the impact of aerosol trajectory history on microbial dynamics. This novel perspective in atmospheric microbial ecology not only challenges existing paradigms but also paves the way for new insights into the consequences of long-range transport on atmospheric microbial community composition.

The categorization of PM transportation pathways into 'North (N)' and 'Southwest (S)' aligns with the findings of Choo et al. (2021), who identified similar long-range aerosol pathways over North Korea and the Yellow Sea (Choo et al., 2021). The cluster 'O' is characterized by its relative stationarity over the inland areas of the Korean peninsula, as described by Lee et al. (2016) and Li et al. (2023). Cluster S was slightly higher in the summation of Na^+ and Cl^- (3.1 %) compared to the other clusters (2.4 % for N and 2.7 % for O), indicating the influence of oceanic aerosols (e.g., sea salt) (Kim et al., 2019). Moreover, the wind speed was low as 1.6 m/s and moderate temperature (8.4 °C) can easily stimulate secondary formation of NH_4NO_3 (Kim et al., 2015; Lee et al., 2016); therefore, the cluster S can be represented the oceanic and secondary formation characteristics. Cluster N, which indicated 'anthropogenic aerosol,' consists of the dominant westerly passed through Beijing-Tianjin-Hebei (BTH) regions showing the highest proportion of carbonaceous aerosols (31.6 % for OC and 3.3 % for EC) along with highest NO_3^- portion (22.5 %). This might be due to air masses passing through urban areas, where is dominant of anthropogenic aerosol from coal-fired power plants and vehicles. The impact of these anthropogenic aerosols generated in the BTH region on the Korean Peninsula has been frequently reported in previous studies (Wang et al., 2005). Cluster N was mainly sampled during winter (the cold season), resulting in favor conditions for secondary formation between NH_3 and HNO_3 which were emitted from the vehicles. High OC and EC concentrations were mainly explained by heating during the cold season (Ghim et al., 2017; Zheng

Table 2
Predicted frequency of LEfSe biomarkers from NCM models and its correlation with physico-chemical variables of $PM_{2.5}$.

Genus	Biomarker[a]	Abundance prediction in NCM[b]				Correlation coefficient[c]											
		All	Cluster N	Cluster S	Cluster O	Temp	Mass	OC	EC	NO_3^-	NH_4^+	SO_4^{2-}	Cl^-	Na^+	K^+	Mg^{2+}	Ca^{2+}
Belliella	N	under[d]	under	neutral	neutral	-0.32											
Nocardiopsis	N/O	neutral	neutral	over	over												0.33
NB1-j	S	neutral	neutral	under	neutral			0.38									
CCD24	S	neutral	neutral	over	neutral												
MND1	S	under	neutral	neutral	over									0.31			
SAR92 clade	S	under	neutral	under	neutral		0.44	0.36	0.35	0.45	0.51	0.45					
Candidatus Ovatusbacter	S	under	neutral	under	-		0.37	0.36		0.42	0.41		0.44				
Chryseobacterium	S	neutral	neutral	under	neutral									0.41	0.31	0.41	
Pirellula	S	neutral	over	neutral	under												
Staphylococcus	S	under	neutral	neutral	neutral		0.33										
Pseudomonas	S	neutral	neutral	over	over												
Thiobacillus	O	under	-[e]	neutral	under	0.43						0.36		0.53	0.46	0.54	0.43
Colwellia	O	under	-	under	under						-0.33	-0.35					

[a]Cluster for which respect genus was revealed as biomarker from LEfSe analysis.
[b]Neutral community models constructed using all samples, cluster N, cluster S, and cluster O, respectively.
[c]Only significant correlation coefficient (Spearman, *rho*) is summarized.
[d]Neutral, well fitted to neutral model; under, under-representative outlier; over, over-representative outlier in NCM.
[e]-, not available due to absence from respect cluster.

et al., 2018). Cluster O consists of a complicated air mass pathway that does not pass through a specific region. As a result, the $PM_{2.5}$ chemical characteristics in cluster O showed a mixture of various emission sources, especially biomass burning (1.5 % for K^+ and 3.4 % for EC) and mineral dust (0.5 % for Ca^{2+} and 0,9 % for Mg^{2+}). As the mean temperature in cluster O was the highest compared to the other clusters, ammonium sulfate ($(NH_4)_2SO_4$) could be a major secondary ion resulting from the photo-disassociation of NH_4NO_3 into NH_3 and HNO_3 (Kim et al., 2015). Therefore, cluster O can be represented as a mixture of aerosols.

The observed differentiation in $PM_{2.5}$-associated bacterial communities across aerial trajectories, coupled with variations in alpha diversity, highlights the complex interplay between stochastic and deterministic forces in microbial community assembly. In particular, the higher alpha diversity and distinct community structure in cluster S, as well as its better fit to the neutral community model, suggested a community assembly primarily influenced by passive dispersal mechanisms, likely shaped by the surrounding marine environments. This finding is in contrast to research, suggesting lower microbial diversity in oceanic aerosols (Archer et al., 2020). The increased bacterial richness in cluster S may be attributed to the dynamics of sea salt aerosolization, which is linearly correlated with ocean surface wind speed (Prijith et al., 2014). This is also evidenced by the higher proportion of over-representative genera in cluster S, indicating that a diverse range of microorganisms were passively dispersed from the surrounding marine environment. This unique interaction could explain the increased microbial diversity despite oceanic influence.

In contrast, clusters N and O, characterized by a less distinct separation and a broader alpha-diversity spectrum, appeared to be more strongly influenced by niche-dependent factors. The negative correlation between microbial diversity and nitrogenous compounds (NH_4^+ and NO_3^-) in cluster N, and the positive correlation with mineral dust indicator (Ca^{2+} and Mg^{2+}) in cluster O, suggests that chemical influences control community composition. These results are consistent with existing research, underscoring the significant contribution of bioaerosols to the atmospheric nitrogen cycle and their interactions with secondary organic aerosols (Archer et al., 2020; Shen and Yao, 2023). This finding highlights the need to consider both natural and anthropogenic factors to understand atmospheric microbial dynamics (Mu et al., 2019; Shen et al., 2016).

This study also provides insights into the roles of particular bacterial taxa as biomarkers in the assembly of bioaerosol communities. The presence of *Pirellula*, Ca. genus NB1-j, and the SAR92 clade in cluster S, which are typical members of coastal environments (Ciraolo et al., 2023; Morris et al., 2006; Stingl et al., 2007), indicate a significant influence of the marine ecosystem on this cluster. The different roles of these biomarkers, as evidenced by their varied fitness in the neutral community model and distinct correlations with chemical factors, suggest a multifaceted interaction with $PM_{2.5}$ components. For example, the DMSP (DiMethyl Sulfonio-Propionate) catabolic activity of Ca. genus SAR92 clade and its correlation with SO_4^{2-} and other secondary organic aerosol highlights its metabolic interactions with these communities (He et al., 2023; Oduro et al., 2012). Over-representative biomarkers in cluster S, such as *Pseudomonas*, show enhanced aerosolization capabilities in marine environments, a notion supported by previous reports on microbial aerosolization rates and capsule production (Michaud et al., 2018). For clusters N and O, the presence of genus *Nocardiopsis* and its correlation with mineral dust indicator (such as Ca^{2+} and Mg^{2+}) is consistent with its known prevalence in desert ecosystems (Alsharif et al., 2020), reinforcing the influence of niche-dependent processes in these clusters. The predominance of under-representative biomarkers in clusters N and O suggests that niche-dependent processes may reduce microbial diversity in these clusters.

Interestingly, *Staphylococcus*, recognized as an opportunistic pathogenic bacterium, was highly dispersed across all clusters, exhibiting a positive correlation with the mass concentration of PM. This indicates that high PM concentration may increase health risks, a notion supported by previous studies (White et al., 2020). Employing $PM_{2.5}$ cluster analysis to predict the spread of potential pathogens such as *Staphylococcus* is critical for public health monitoring and risk assessment. For instance, an assessment based on urban aerosol samples from kindergartens revealed seasonal variations in health risks associated with pathogenic bacterial assembly mechanisms (Li et al., 2022). Implementing such approaches can aid the development of targeted air quality management and early warning systems, particularly in urban settings or areas prone to dust storms.

Although this study provides important insights into the assembly mechanisms of microbial communities in bioaerosols and their interactions with the physicochemical dynamics of the atmosphere, there are still many gaps that need to be filled and researched further. A primary limitation is the spatial and temporal variability inherent in bioaerosol studies. Our sampling, which was restricted to a single location over a limited timeframe, may not have fully captured the complex and dynamic nature of bioaerosol transport and microbial diversity across various atmospheric conditions and seasons. This highlights the need for more comprehensive and diverse sampling strategies in future studies to gain a comprehensive understanding of the spatiotemporal dynamics of bioaerosol communities. Furthermore, the current focus on bacterial communities overlooks the roles of other microbial entities such as fungi, viruses, and microeukaryotes, which are integral to the atmospheric microbiome. Incorporating these groups into future research could provide a more holistic view of atmospheric microbial ecology. The integration of metagenomic and metatranscriptomic approaches would be beneficial to further elucidate the functional and metabolic profiles of these microbial communities. Such approaches could improve our understanding of the ecological roles and impacts of bioaerosols, particularly in terms of atmospheric processes and public health. Finally, this study opens the door for further investigations into how anthropogenic pollutants and climate change may affect microbial communities in bioaerosols. These significantly affect the chemical composition of organic carbon, which is vital for microbial resource availability. This importance highlights the need for detailed studies on how these changes influence bioaerosol composition, function, and dispersal, with recent FT-ICR-MS advancements offering a way to closely examine bioaerosol organic matter's chemical characteristics (Zhang et al., 2024). With current environmental challenges, it is critical to understand the impact of these factors on bioaerosol composition, function, and dispersal patterns. Future research in these areas will advance understanding of atmospheric microbial ecology and inform strategies for air quality management and public health protection in the face of global environmental change.

5. Conclusion

This study advances our understanding of the complex dynamics that control the microbial community assembly and physicochemical interactions in atmospheric bioaerosols. Through a detailed analysis of samples collected over a two-year period, we clarified the important role of both deterministic and stochastic processes in shaping these communities, influenced by their different aerial trajectories and complex interaction with environmental factors. Our results highlight the importance of geographic origin and atmospheric journey in determining the composition and diversity of microbial communities in bioaerosols. The use of advanced molecular techniques and neutral community model analyses allowed us to analyze the subtle balance between passive dispersal mechanisms and niche-dependent factors and to highlight the pronounced associations between environmental conditions and microbial interactions in the atmosphere. Furthermore, the different microbial signatures associated with different aerial trajectories underscore the potential of bioaerosols as indicators of air quality and as vectors for pathogen spread, which has significant implications for environmental monitoring and public health risk assessments. This

opens new avenues for research and provides a foundation for future studies aimed at understanding the environmental and health impacts of bioaerosols in the atmosphere.

CRediT authorship contribution statement

Jin-Kyung Hong: Writing – review & editing, Writing – original draft, Methodology, Investigation, Funding acquisition, Formal analysis, Data curation. **Yongjoo Choi:** Writing – review & editing, Methodology, Investigation, Conceptualization. **Seokhyun Ahn:** Investigation. **Jeonghwan Kim:** Investigation. **Dong Jin Yang:** Investigation. **Jongwon Heo:** Investigation. **Jae-Chang Cho:** Writing – review & editing. **Tae Kwon Lee:** Writing – review & editing, Writing – original draft, Supervision, Funding acquisition, Conceptualization.

Declaration of competing interest

The authors declare no conflict of interest.

Data availability

Data will be made available on request.

Acknowledgements

This project was conducted with support from the National Research Foundation of Korea (NRF-2020R1F1A1071285) funded by the Ministry of Science and Information and Communication Technology (MSIT), and also supported by the Animal and Plant Quarantine Agency (Z-1543081-2023-25-0101).

Appendix A. Supplementary data

Supplementary data to this article can be found online at https://doi.org/10.1016/j.scitotenv.2024.172736.

References

Alsharif, W., Saad, M.M., Hirt, H., 2020. Desert microbes for boosting sustainable agriculture in extreme environments. Front. Microbiol. 11, 1666.
Amir, A., McDonald, D., Navas-Molina, J.A., Kopylova, E., Morton, J.T., Zech Xu, Z., Kightley, E.P., Thompson, L.R., Hyde, E.R., Gonzalez, A., Knight, R., 2017. Deblur rapidly resolves single-nucleotide community sequence patterns. mSystems 2 (2).
Archer, S.D.J., Lee, K.C., Caruso, T., King-Miaow, K., Harvey, M., Huang, D., Wainwright, B.J., Pointing, S.B., 2020. Air mass source determines airborne microbial diversity at the ocean-atmosphere interface of the Great Barrier Reef marine ecosystem. ISME J. 14 (3), 871–876.
Bokulich, N.A., Dillon, M.R., Bolyen, E., Kaehler, B.D., Huttley, G.A., Caporaso, J.G., 2018. q2-sample-classifier: machine-learning tools for microbiome classification and regression. J. Open Res. Softw. 3 (30).
Bolyen, E., Rideout, J.R., Dillon, M.R., Bokulich, N.A., Abnet, C.C., Al-Ghalith, G.A., Alexander, H., Alm, E.J., Arumugam, M., Asnicar, F., Bai, Y., Bisanz, J.E., Bittinger, K., Brejnrod, A., Brislawn, C.J., Brown, C.T., Callahan, B.J., Caraballo-Rodriguez, A.M., Chase, J., Cope, E.K., Da Silva, R., Diener, C., Dorrestein, P.C., Douglas, G.M., Durall, D.M., Duvallet, C., Edwardson, C.F., Ernst, M., Estaki, M., Fouquier, J., Gauglitz, J.M., Gibbons, S.M., Gibson, D.L., Gonzalez, A., Gorlick, K., Guo, J., Hillmann, B., Holmes, S., Holste, H., Huttenhower, C., Huttley, G.A., Janssen, S., Jarmusch, A.K., Jiang, L., Kaehler, B.D., Kang, K.B., Keefe, C.R., Keim, P., Kelley, S.T., Knights, D., Koester, I., Kosciolek, T., Kreps, J., Langille, M.G.I., Lee, J., Ley, R., Liu, Y.X., Loftfield, E., Lozupone, C., Maher, M., Marotz, C., Martin, B.D., McDonald, D., McIver, L.J., Melnik, A.V., Metcalf, J.L., Morgan, S.C., Morton, J.T., Naimey, A.T., Navas-Molina, J.A., Nothias, L.F., Orchanian, S.B., Pearson, T., Peoples, S.L., Petras, D., Preuss, M.L., Pruesse, E., Rasmussen, L.B., Rivers, A., Robeson 2nd, M.S., Rosenthal, P., Segata, N., Shaffer, M., Shiffer, A., Sinha, R., Song, S.J., Spear, J.R., Swafford, A.D., Thompson, L.R., Torres, P.J., Trinh, P., Tripathi, A., Turnbaugh, P.J., Ul-Hasan, S., van der Hooft, J.J.J., Vargas, F., Vazquez-Baeza, Y., Vogtmann, E., von Hippel, M., Walters, W., Wan, Y., Wang, M., Warren, J., Weber, K.C., Williamson, C.H.D., Willis, A.D., Xu, Z.Z., Zaneveld, J.R., Zhang, Y., Zhu, Q., Knight, R., Caporaso, J.G., 2019. Reproducible, interactive, scalable and extensible microbiome data science using QIIME 2. Nat. Biotechnol. 37 (8), 852–857.
Carslaw, D.C., 2019. The Openair Manual - Open-Source Tools for Analysing Air Pollution Data. Manual for Version 2.6–6. University of York.
Chen, W., Ren, K., Isabwe, A., Chen, H., Liu, M., Yang, J., 2019. Stochastic processes shape microeukaryotic community assembly in a subtropical river across wet and dry seasons. Microbiome 7 (1), 138.
Choi, Y., Kanaya, Y., Park, S.-M., Matsuki, A., Sadanaga, Y., Kim, S.-W., Uno, I., Pan, X., Lee, M., Kim, H., 2020. Regional variability in black carbon and carbon monoxide ratio from long-term observations over East Asia: assessment of representativeness for black carbon (BC) and carbon monoxide (CO) emission inventories. Atmos. Chem. Phys. 20 (1), 83–98.
Choo, G.-H., Lee, K., Seo, J., Kim, S.-Y., Lee, D.-W., Shin, H.-J., 2021. Optical and chemical properties of long-range transported aerosols using satellite and ground-based observations over Seoul, South Korea. Atmos. Environ. 246, 118024.
Ciraolo, A.C., Snelgrove, P.V., Algar, C.K., 2023. Habitat heterogeneity effects on microbial communities of the Gulf of Maine. Deep Sea Res. Part I Oceanogr. Res. Pap. 197, 104074.
Draxler, R., Stunder, B., Rolph, G., Stein, A., Taylor, A., 2018. HYSPLIT4 User's Guide, Version 4.
Duchaine, C., Roy, C.J., 2022. Bioaerosols and airborne transmission: integrating biological complexity into our perspective. Sci. Total Environ. 825, 154117.
Dussud, C., Meistertzheim, A.L., Conan, P., Pujo-Pay, M., George, M., Fabre, P., Coudane, J., Higgs, P., Elineau, A., Pedrotti, M.L., Gorsky, G., Ghiglione, J.F., 2018. Evidence of niche partitioning among bacteria living on plastics, organic particles and surrounding seawaters. Environ. Pollut. 236, 807–816.
Feng, Z., Shen, H., Nie, Y., Wu, X.L., 2021. The impacts of the occupants on the bacterial communities of classrooms. Curr. Microbiol. 78 (5), 2112–2121.
Ghim, Y.S., Kim, J.Y., Chang, Y.-S., 2017. Concentration variations in particulate matter in Seoul associated with Asian dust and smog episodes. Aerosol Air Qual. Res. 17 (12), 3128–3140.
Gong, J., Qi, J., E, B., Yin, Y., Gao, D., 2020. Concentration, viability and size distribution of bacteria in atmospheric bioaerosols under different types of pollution. Environ. Pollut. 257, 113485.
Hamilton, K.A., Hamilton, M.T., Johnson, W., Jjemba, P., Bukhari, Z., LeChevallier, M., Haas, C.N., 2018. Health risks from exposure to Legionella in reclaimed water aerosols: toilet flushing, spray irrigation, and cooling towers. Water Res. 134, 261–279.
He, X.Y., Liu, N.H., Liu, J.Q., Peng, M., Teng, Z.J., Gu, T.J., Chen, X.L., Chen, Y., Wang, P., Li, C.Y., Todd, J.D., Zhang, Y.Z., Zhang, X.Y., 2023. SAR92 clade bacteria are potentially important DMSP degraders and sources of climate-active gases in marine environments. mBio e0146723.
Hong, J.K., Cho, J.C., 2015. Environmental variables shaping the ecological niche of Thaumarchaeota in soil: direct and indirect causal effects. PLoS One 10 (8), e0133763.
Jiang, W., Liang, P., Wang, B., Fang, J., Lang, J., Tian, G., Jiang, J., Zhu, T.F., 2015. Optimized DNA extraction and metagenomic sequencing of airborne microbial communities. Nat. Protoc. 10 (5), 768–779.
Jiang, X., Wang, C., Guo, J., Hou, J., Guo, X., Zhang, H., Tan, J., Li, M., Li, X., Zhu, H., 2022. Global meta-analysis of airborne bacterial communities and associations with anthropogenic activities. Environ. Sci. Technol. 56 (14), 9891–9902.
Kanaya, Y., Pan, X., Miyakawa, T., Komazaki, Y., Taketani, F., Uno, I., Kondo, Y., 2016. Long-term observations of black carbon mass concentrations at Fukue Island, western Japan, during 2009–2015: constraining wet removal rates and emission strengths from East Asia. Atmos. Chem. Phys. 16 (16), 10689–10705.
Kim, C.H., Choi, Y., Ghim, Y.S., 2015. Characterization of volatilization of filter-sampled PM2.5 semi-volatile inorganic ions using a backup filter and denuders. Aerosol Air Qual. Res. 15 (3), 814–820.
Kim, H.J., Lee, T., Park, T., Park, G., Collett, J.L., Park, K., Ahn, J.Y., Ban, J., Kang, S., Kim, K., 2019. Ship-borne observations of sea fog and rain chemistry over the North and South Pacific Ocean. J. Atmos. Chem. 76, 315–326.
Lee, Y.H., Choi, Y., Ghim, Y.S., 2016. Classification of diurnal patterns of particulate inorganic ions downwind of metropolitan Seoul. Environ. Sci. Pollut. Res. 23, 8917–8928.
Li, H., Liu, P.Q., Luo, Q.P., Ma, J.J., Yang, X.R., Yan, Y., Su, J.Q., Zhu, Y.G., 2022. Spatiotemporal variations of microbial assembly, interaction, and potential risk in urban dust. Environ. Int. 170, 107577.
Li, H., Hong, Y.W., Gao, M.K., An, X.L., Yang, X.R., Zhu, Y.G., Chen, J.S., Su, J.Q., 2023. Distinct responses of airborne abundant and rare microbial communities to atmospheric changes associated with Chinese New Year. iMeta e140.
Michaud, J.M., Thompson, L.R., Kaul, D., Espinoza, J.L., Richter, R.A., Xu, Z.Z., Lee, C., Pham, K.M., Beall, C.M., Malfatti, F., Azam, F., Knight, R., Burkart, M.D., Dupont, C. L., Prather, K.A., 2018. Taxon-specific aerosolization of bacteria and viruses in an experimental ocean-atmosphere mesocosm. Nat. Commun. 9 (1), 2017.
Morris, R.M., Longnecker, K., Giovannoni, S.J., 2006. Pirellula and OM43 are among the dominant lineages identified in an Oregon coast diatom bloom. Environ. Microbiol. 8 (8), 1361–1370.
Mu, L., Zheng, L., Liang, M., Tian, M., Li, X., Jing, D., 2019. Characterization and source analysis of water-soluble ions in atmospheric particles in Jinzhong, China. Aerosol Air Qual. Res. 19 (11), 2396–2409.
Oduro, H., Van Alstyne, K.L., Farquhar, J., 2012. Sulfur isotope variability of oceanic DMSP generation and its contributions to marine biogenic sulfur emissions. Proc. Natl. Acad. Sci. U. S. A. 109 (23), 9012–9016.
Oksanen, J., Blanchet, F.G., Friendly, M., Kindt, R., Legendre, P., McGlinn, D., Minchin, P.R., O'hara, R., Simpson, G.L., Solymos, P., 2019. Package 'Vegan'. Community Ecology Package, Version 2(9).
Peipoch, M., Miller, S.R., Antao, T.R., Valett, H.M., 2019. Niche partitioning of microbial communities in riverine floodplains. Sci. Rep. 9 (1), 16384.
Prijith, S., Aloysius, M., Mohan, M., 2014. Relationship between wind speed and sea salt aerosol production: a new approach. J. Atmos. Sol.-Terr. Phys. 108, 34–40.

Rideout, J.R., He, Y., Navas-Molina, J.A., Walters, W.A., Ursell, L.K., Gibbons, S.M., Chase, J., McDonald, D., Gonzalez, A., Robbins-Pianka, A., Clemente, J.C., Gilbert, J. A., Huse, S.M., Zhou, H.W., Knight, R., Caporaso, J.G., 2014. Subsampled open-reference clustering creates consistent, comprehensive OTU definitions and scales to billions of sequences. PeerJ 2, e545.
Segata, N., Izard, J., Waldron, L., Gevers, D., Miropolsky, L., Garrett, W.S., Huttenhower, C., 2011. Metagenomic biomarker discovery and explanation. Genome Biol. 12 (6), R60.
Shen, F., Yao, M., 2023. Bioaerosol nexus of air quality, climate system and human health. Nat. Sci. Open 2 (4), 20220050.
Shen, Z., Sun, J., Cao, J., Zhang, L., Zhang, Q., Lei, Y., Gao, J., Huang, R.-J., Liu, S., Huang, Y., 2016. Chemical profiles of urban fugitive dust PM2. 5 samples in Northern Chinese cities. Sci. Total Environ. 569, 619–626.
Sloan, W.T., Lunn, M., Woodcock, S., Head, I.M., Nee, S., Curtis, T.P., 2006. Quantifying the roles of immigration and chance in shaping prokaryote community structure. Environ. Microbiol. 8 (4), 732–740.
Smets, W., Moretti, S., Denys, S., Lebeer, S., 2016. Airborne bacteria in the atmosphere: presence, purpose, and potential. Atmos. Environ. 139, 214–221.
Stingl, U., Desiderio, R.A., Cho, J.C., Vergin, K.L., Giovannoni, S.J., 2007. The SAR92 clade: an abundant coastal clade of culturable marine bacteria possessing proteorhodopsin. Appl. Environ. Microbiol. 73 (7), 2290–2296.
Tripathi, B.M., Stegen, J.C., Kim, M., Dong, K., Adams, J.M., Lee, Y.K., 2018. Soil pH mediates the balance between stochastic and deterministic assembly of bacteria. ISME J. 12 (4), 1072–1083.
Wang, Y., Zhuang, G., Tang, A., Yuan, H., Sun, Y., Chen, S., Zheng, A., 2005. The ion chemistry and the source of PM2.5 aerosol in Beijing. Atmos. Environ. 39 (21), 3771–3784.
Wang, K., Razzano, M., Mou, X., 2020. Cyanobacterial blooms alter the relative importance of neutral and selective processes in assembling freshwater bacterioplankton community. Sci. Total Environ. 706, 135724.
White, J.K., Nielsen, J.L., Larsen, C.M., Madsen, A.M., 2020. Impact of dust on airborne Staphylococcus aureus' viability, culturability, inflammogenicity, and biofilm forming capacity. Int. J. Hyg. Environ. Health 230, 113608.
Wurie, F.B., Lawn, S.D., Booth, H., Sonnenberg, P., Hayward, A.C., 2016. Bioaerosol production by patients with tuberculosis during normal tidal breathing: implications for transmission risk. Thorax 71 (6), 549–554.
Zhai, Y., Li, X., Wang, T., Wang, B., Li, C., Zeng, G., 2018. A review on airborne microorganisms in particulate matters: composition, characteristics and influence factors. Environ. Int. 113, 74–90.
Zhang, S., Liang, Z., Wang, X., Ye, Z., Li, G., An, T., 2023. Bioaerosols in an industrial park and the adjacent houses: dispersal between indoor/outdoor, the impact of air purifier, and health risk reduction. Environ. Int. 172, 107778.
Zhang, G., Lou, M., Xu, J., Li, Y., Zhou, J., Guo, H., Qu, G., Wang, T., Jia, H., Zhu, L., 2024. Molecular insights into microbial transformation of bioaerosol-derived dissolved organic matter discharged from wastewater treatment plant. Environ. Int. 183, 108404.
Zhao, J., Jin, L., Wu, D., Xie, J.W., Li, J., Fu, X.W., Cong, Z.Y., Fu, P.Q., Zhang, Y., Luo, X. S., Feng, X.B., Zhang, G., Tiedje, J.M., Li, X.D., 2022. Global airborne bacterial community-interactions with Earth's microbiomes and anthropogenic activities. Proc. Natl. Acad. Sci. U. S. A. 119 (42), e2204465119.
Zheng, B., Tong, D., Li, M., Liu, F., Hong, C., Geng, G., Li, H., Li, X., Peng, L., Qi, J., 2018. Trends in China's anthropogenic emissions since 2010 as the consequence of clean air actions. Atmos. Chem. Phys. 18 (19), 14095–14111.
Zhou, J., Ning, D., 2017. Stochastic community assembly: does it matter in microbial ecology? Microbiol. Mol. Biol. Rev. 81, e00002-17.
Zhou, F., Niu, M., Zheng, Y., Sun, Y., Wu, Y., Zhu, T., Shen, F., 2021. Impact of outdoor air on indoor airborne microbiome under hazy air pollution: a case study in winter Beijing. J. Aerosol Sci. 156, 105798.